The effects of velocity and nitrate on *Phormidium* accrual cycles: a stream mesocosm experiment

Tara G. McAllister[1,6], Susanna A. Wood[2,7], Michelle J. Greenwood[3,8], Felix Broghammer[4,9], and Ian Hawes[5,10]

[1]Waterways Centre for Freshwater Management, University of Canterbury, Private Bag 4800, Christchurch, New Zealand
[2]Cawthron Institute, Private Bag 2, Nelson, New Zealand
[3]National Institute of Water and Atmospheric Research, P.O. Box 8602, Christchurch, New Zealand
[4]Faculty of Biology, Technische Universität Dresden, Zellescher Weg 20b, 01217 Dresden, Germany
[5]Coastal Marine Field Station, University of Waikato, 58 Cross Road, Tauranga, New Zealand

Abstract: Proliferations of benthic cyanobacteria in the genus *Phormidium* are a global concern because of their increasing prevalence and ability to produce harmful toxins. Most studies have been observational and have linked physicochemical variables to *Phormidium* cover measured at the reach scale. Authors of these studies have alluded to nutrients and flow as key factors in accrual. Our goal was to use an experimental approach to examine how changes in velocity and NO_3^- concentrations influence *Phormidium* accrual. We hypothesized that: 1) *Phormidium* biomass accrual would be positively correlated with stream velocity; 2) biomass accrual would be positively related to NO_3^- concentration, which would have a stronger effect during early accrual; 3) an NO_3^- × velocity interaction would arise from saturation of accrual at high NO_3^- and high velocity; and 4) the probability of detachment would increase with decreasing velocity. We assessed mat expansion, biomass (as phycoerythrin and chlorophyll *a* [Chl *a*] concentrations, and biovolume), and algal assemblage composition in flow-through channel mesocosms for 16 d. We crossed 2 velocity treatments (0.1 and 0.2 m/s, slow and fast, respectively) with 3 NO_3^- treatments (0.02, 0.1, and 0.4 mg/L, ambient, medium, and high, respectively). Velocity was positively correlated with all measures of *Phormidium* biomass, but patch expansion rates increased at similar rates across all treatments. NO_3^- had no effect during early accrual, but phycoerythrin concentrations increased with increasing NO_3^- in fast-velocity treatments. At the end of the experiment, patch size was greater in the high-velocity treatments because of a greater number of partial or full patch detachments in slow-velocity treatments. These results suggest that NO_3^- concentrations do not affect *Phormidium* expansion and detachment, but may be important during colonization (not investigated), and that mat expansion occurs at a similar rate regardless of velocity, but termination of accrual cycles occurs earlier in slow velocities.

Key words: *Phormidium*, nitrate, velocity, accrual cycles, patch expansion, sloughing

Landuse change is one of the main drivers of ecological degradation in lotic ecosystems worldwide (Vörösmarty et al. 2010). Agricultural, forest, and urban land use affect nutrient delivery to waterways and increase water extraction for both irrigation and drinking water purposes (Baron et al. 2002, Walling and Fang 2003, Weijters et al. 2009). Resultant changes to stream ecosystems include augmented nutrient concentrations and alterations in the volume and seasonality of flow. These 2 globally important stressors are likely to affect benthic algal communities in complex and interactive ways. In lakes, enhanced nutrient loadings frequently lead to proliferations of toxic cyanobacteria (Oliver et al. 2012), and concern exists that alterations of streams' ecosystems because of landuse change and intensification may create conditions that favor the dominance of toxin-producing benthic cyanobacterial species and excessive biomass accrual (McAllister et al. 2016).

Phormidium is a benthic mat-forming cyanobacterial genus that produces a variety of cyanotoxins and is becoming increasingly problematic in cobble-bed rivers worldwide (Aboal et al. 2002, Gugger et al. 2005, Quiblier et al. 2013, Fetscher et al. 2015, McAllister et al. 2016). Animal

E-mail addresses: [6]tara.mcallister0@gmail.com; [7]susie.wood@cawthron.org.nz; [8]michelle.greenwood@niwa.co.nz; [9]broghammerfelix@gmail.com; [10]ian.hawes@waikato.ac.nz

DOI: 10.1086/699204. Received 17 January 2018; Accepted 29 March 2018; Published online 27 June 2018.
Freshwater Science. 2018. 37(3):496–509.

toxicosis events attributed to *Phormidium*-dominated mats (hereafter *Phormidium*) have been reported in France, Scotland, Switzerland, The Netherlands, the USA, and New Zealand (Edwards et al. 1992, Mez et al. 1997, Hamill 2001, Gugger et al. 2005, Wood et al. 2007, Faassen et al. 2012). Previous research on the ecology of *Phormidium* has been largely limited to observation-based studies identifying correlations between physicochemical factors and reach-scale *Phormidium* dynamics. These observational studies have implicated nutrients, flow, and sediment as potentially linked to accrual dynamics (Heath et al. 2011, Wood et al. 2015, 2017, McAllister et al. 2018). Causal and interactive relationships of physicochemical factors driving proliferations on a finer scale and in a more controlled setting must be investigated to elucidate mechanistic links. Identification of driving variables may be complicated by the nature of the *Phormidium* accrual cycle, which involves colonization, initiation of a benthic mat, growth via patch expansion, and eventual detachment. Each of these successional phases may respond differently to water velocity and nutrient concentrations (McAllister et al. 2016).

Heath et al. (2015) created velocity-based habitat-suitability curves for *Phormidium*, which indicated that it was found most frequently at velocities of 0.6 to 1.1 m/s and was rare at higher or lower velocities. Other researchers have confirmed that *Phormidium* appears to be rheophilic and that early colonization and heightened growth tends to occur in reaches with relatively high velocity (Hart et al. 2013, Bouma-Gregson 2015, Heath et al. 2015). At the upper end of its velocity range, abrasion may limit accrual but at low velocity, autogenic detachment may be more important. Several mass-detachment events have been documented under low velocities (Sabater et al. 2003, McAllister et al. 2018). These events were attributed to excessive buoyancy induced by bubble formation during photosynthesis. Low velocity may be disadvantageous because of formation of thicker boundary layers, which limit the flux of O_2 between the mat and water, thereby facilitating gas bubble formation during photosynthesis (Boulêtreau et al. 2006, Bouma-Gregson et al. 2017).

Phormidium proliferations can occur across a range of nutrient concentrations. In New Zealand, proliferations of *Phormidium* consistently occur at dissolved reactive P (DRP) concentrations <0.01 mg/L (Wood et al. 2015, 2017, McAllister et al. 2016), whereas in Spain, *Phormidium autumnale* is prevalent in hypertrophic systems (Loza et al. 2013). Wood et al. (2017) suggested a lower limit of water-column dissolved inorganic N (DIN) concentrations for proliferation of *Phormidium* of ~0.1 mg/L, but proliferations have been observed in NO_3^- concentrations <0.02 mg/L (Wood et al. 2017, McAllister et al. 2018). The ability to accumulate biomass under low nutrient concentrations is a well-established trait of benthic microbial mats (Bonilla et al. 2005). Investigators have suggested that elevated NO_3^- concentrations enhance *Phormidium* growth during early accrual stages, but that internal mat nutrient-cycling processes in established mats allow it to grow independently of water-column nutrient concentrations (McAllister et al. 2016, 2018, Wood et al. 2017). Studies of the effect of NO_3^- on *Phormidium* growth have been limited to laboratory-culture-based (Heath et al. 2014, 2016) and observational studies (Heath et al. 2011, Wood et al. 2017, McAllister et al. 2018). Observational studies are complicated by covariation of other physicochemical factors that make extraction of meaningful relationships difficult. Furthermore, molecular studies have shown that *Phormidium* isolated from New Zealand rivers does not have the ability to fix N (Heath 2009), but highlighted that diverse bacterial communities exist within *Phormidium* mats, and some of these bacteria are capable of N fixation (Brasell et al. 2015). If N fixation becomes significant as mats mature, the importance of water-column N may decline as mat biomass accrues.

Velocity and nutrients are likely to interact and affect *Phormidium* accrual dynamics, particularly where growth requires fluxes of nutrients from water to the mat. The thick and dense nature of *Phormidium* mats may facilitate development of boundary layers (Larned et al. 2004), which represent a barrier to nutrient uptake and delivery (Biggs et al. 1998). Consequently, rates of biomass accrual may be nutrient-limited under low-flow conditions (Hart et al. 2013). The combination of low velocity and low nutrients could combine to limit *Phormidium* growth, whereas under higher velocities or higher NO_3^- concentrations, any limitation of *Phormidium* growth may be offset by increased delivery of nutrients across the boundary layer.

We used streamside experimental mesocosms to investigate the interactive effects of velocity and NO_3^- concentrations on the expansion, biomass accrual, and detachment of *Phormidium*. In this experiment, we seeded cobbles with *Phormidium*, which allowed us to standardize the colonization step of the accrual cycle and to focus on the accrual and detachment phases. We tested the following hypotheses: 1) *Phormidium* biomass accrual will be positively correlated with stream velocity; 2) biomass accrual will be positively related to NO_3^- concentration, and NO_3^- will have a stronger effect during early accrual; 3) NO_3^- and velocity will interact such that accrual is saturated at high NO_3^- and high velocity because of nutrient delivery; and 4) the probability of detachment will increase with decreasing velocity because of accumulation of O_2 bubbles within mats.

METHODS

Experimental facility and design

We conducted the experiment from 2 to 18 April 2016 in outdoor, channel mesocosms (Fig. 1A). The experimental facility was beside an irrigation race fed by the Kowai River, South Island, New Zealand (lat 43°19′54.92″S, long 171°53′6.19″E). Ambient water from the Kowai River con-

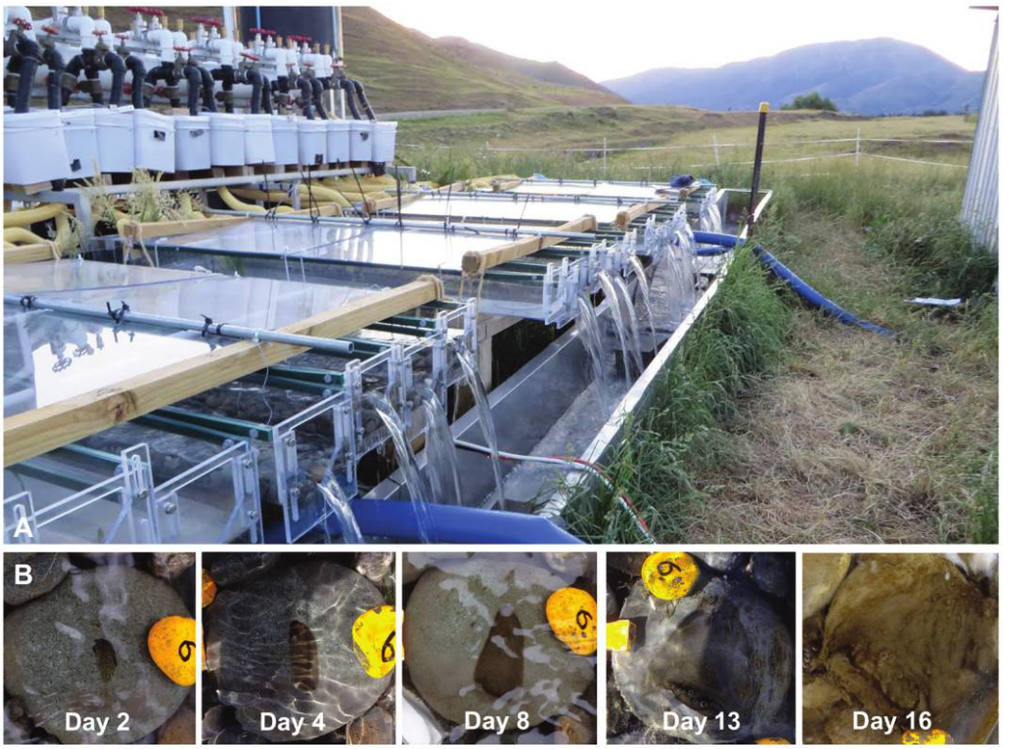

Figure 1. Photograph showing the experimental set up (A) and an example of *Phormidium* expansion in fast velocity/medium NO_3^- treatment (B). A hole (4 mm in depth and diameter) was drilled into the center of each cobble, which was then seeded with homogenized *Phormidium* mats.

tained low concentrations of NO_3^- (0.015–0.042 mg/L), which allowed us to undertake NO_3^- amendments.

We pumped water from the irrigation race in the Kowai River into 2 separate 500-L header tanks and then gravity-fed it to 10-L mixing tanks (n = 18). We added nutrients (NO_3^- and PO_4^{3-}) constantly to individual mixing tanks from stock solutions ($NaNO_3$ and $NaHPO_4{\cdot}2H_2O$) via a Masterflex L/S multichannel peristaltic pump (Cole–Palmer Instrument Company, Vernon Hills, Illinois). Water from the intermediate tanks then flowed into 18 channels (2 m long × 0.2 m wide × 0.2 m deep) that we constructed according to Bothwell (1988). We regulated the flow into each channel by control valves at the outlet of the mixing tanks and altered velocity by changing the water depth and slope of individual channels. Each channel contained a layer of small–medium-sized gravel (~5–7 cm^2).

We crossed 3 NO_3^- treatments (ambient, medium, high) with 2 velocity treatments (slow and fast), resulting in 6 treatments, each replicated 3 times (SA = slow velocity/ambient NO_3^-, FA = fast velocity/ambient NO_3^-, SM = slow velocity/medium NO_3^-, FM = fast velocity/medium NO_3^-, SH = slow velocity/high NO_3^-, and FH = fast velocity/high NO_3^-). NO_3^- target concentrations of 0.02 mg/L (ambient), 0.2 mg/L (medium) and 0.4 mg/L (high) (see Table 1 for realized concentrations) were selected to represent the gradient of NO_3^- observed in some lowland streams on the Canterbury Plains, New Zealand, and concentrations under which *Phormidium* proliferations have occurred (McAllister et al. 2016). We added PO_4^{3-} to all channels to a target concentration of 0.01 mg/L, which was considered to be in excess of requirements for *Phormidium* growth. The velocity levels achieved in our experiment were limited by mesocosm design and pump capabilities. Fast treatments had a mean velocity of 0.2 m/s and a mean depth of 0.05 m, whereas slow treatments had a mean velocity of 0.07 m/s and a mean depth of 0.08 m. We estimated velocity as:

$$V = \frac{Q}{A}, \qquad \text{(Eq. 1)}$$

where V is velocity, Q is discharge, and A is the cross-sectional area of the mesocosms.

We further characterized velocity treatments with clod cards, which is a method for comparing relative velocity by measuring the dissolution rate of uniform blocks of plaster of Paris (Larned and Stimson 1996). Higher rates of dissolution indicate a higher-velocity environment. We molded clods in ice-cube trays, and dried, weighed, and then deployed them for 48 h in replicates of 3 in each mesocosm on 4 occasions over the experimental period. After deployment, we dried clods at 60°C for 48 h and reweighed them.

Table 1. Mean (SD) concentrations of NO_3^- + NO_2^--N and dissolved reactive P (DRP) measured in water samples (n = 3) collected from each mesocosm (n = 18) on days 4, 11, and 16. SA = slow velocity/ambient NO_3^-, FA = fast velocity/ambient NO_3^-, SM = slow velocity/medium NO_3^-, FM = fast velocity/medium NO_3^-, SH = slow velocity/high NO_3^-, FH = fast velocity/high NO_3^-. Slow velocity = 0.1 m/s, fast velocity = 0.2 m/s.

		Nutrient concentration (mg/L)	
Treatment	Day	NO_3^- + NO_2^--N	DRP
FA	4	0.026 (0.004)	0.011 (0.003)
	11	0.038 (0.017)	0.009 (0.001)
	16	0.016 (0.001)	0.010 (0.003)
SA	4	0.026 (0.004)	0.010 (0.001)
	11	0.042 (0.005)	0.008 (0.001)
	16	0.015 (0.001)	0.010 (0.001)
FM	4	0.132 (0.046)	0.012 (0.003)
	11	0.141 (0.034)	0.012 (0.005)
	16	0.089 (0.017)	0.011 (0.001)
SM	4	0.107 (0.018)	0.012 (0.002)
	11	0.133 (0.006)	0.009 (0.001)
	16	0.115 (0.042)	0.009 (0.001)
FH	4	0.494 (0.225)	0.011 (0.003)
	11	0.379 (0.045)	0.008 (0.001)
	16	0.406 (0.054)	0.009 (0.001)
SH	4	0.486 (0.189)	0.014 (0.004)
	11	0.485 (0.167)	0.009 (0.001)
	16	0.375 (0.010)	0.009 (0.001)

Mass losses were corrected for dissolution in still water by conducting a still-water deployment according to Thompson and Glenn (1994) before calculating the rate of dissolution.

We collected a total of 324 cobbles with surface areas between 60 and 90 cm^2 from the Ōpihi River at State Highway 1 (lat 44°15′49″S, long 171°16′10″E). We also collected *Phormidium* mats from the Ōpihi River on day 0 of the experiment. This site had average DIN and DRP concentrations of 0.167 and 0.02 mg/L, respectively (McAllister et al. 2018). On day 0, we scrubbed the cobbles and drilled a single hole (4 mm in depth and diameter) into the center of each cobble. We filled the hole with *Phormidium*-dominated mats homogenized with a handheld blender (Kenwood, Hampshire, UK; Fig. 1B). We placed 18 cobbles in each channel.

We measured water temperature in 5 mesocosms every 15 min during the experimental period using thermistors connected to a Starlogger datalogger (NIWA Instrument Systems, Christchurch, New Zealand).

Sample collection

We followed *Phormidium* patch expansion on seeded cobbles by photographing cobbles every 2 to 3 d throughout the experimental period and calculating patch area using ImageJ (National Institutes of Health, Bethesda, Maryland). We checked images for distortion with a calibrated target imaged from the same distance, and no effect was apparent.

For biomass estimates, we randomly selected 3 cobbles from each mesocosm. We measured chlorophyll *a* (Chl *a*), biovolume, and algal composition on cobbles on days 4, 11, and 16. On day 16, we also collected samples to measure phycoerythrin concentrations. We scrubbed the upward-facing surface area of each cobble with a nylon brush with 50 mL of deionized water for 2 min and then homogenized the slurry with a handheld blender (Kenwood, London, UK). We filtered aliquots (10 mL) for Chl *a* and phycoerythrin through GF/C filters (Whatman, Maidstone, UK) and froze them (−20°C) until later analysis. We combined the remainder of the samples from the 3 cobbles in each mesocosm and mixed them before collecting a 2-mL subsample for taxonomic assessments and biovolume calculations. We preserved the subsample in Lugol's iodine and stored it at 4°C until analysis. We estimated the upward-facing surface areas of sampled cobbles by molding and trimming a single layer of Al foil to the surface area of the cobble and then weighing the foil. We used a calibration curve based on foil of known surface area to convert the mass of foil to surface area.

We collected water samples for both NO_3^- + NO_2^--N and DRP from the outflow of each mesocosm on days 4, 11, and 16 to confirm nutrient concentrations. We filtered samples on site: NO_3^- + NO_2^--N samples through GF/C filters and DRP samples through 0.45-μm membrane filters (Millipore, Burlington, Massachusetts). We transported water samples on ice and stored them at –20°C until further analysis.

Laboratory analysis

We extracted phycoerythrin in 5 mL of potassium phosphate buffer (0.1 M, pH = 6.8) and mechanically homogenized the sample with a Teflon™ and glass homogenizer. We stored samples at 4°C for 24 h before filtering them (GF/C) and measuring phycoerythrin concentrations with a fluorometer (Aquaflor; Turner Designs, San Jose, California). We calibrated the fluorescence output by creating a dilution series of an extract of a *Phormidium* mat sample containing sufficient phycoerythrin to allow quantification using spectrometric absorbance. We converted absorbance to concentration with a specific absorption coefficient of 300,000 taken from Bryant et al. (1976).

We extracted Chl *a* from material collected on filters in boiling ethanol (96%; 2 mL, 2 min). After storage at 4°C for 24 h, we centrifuged the samples (3000*g*, 15 min) and measured absorbance spectrophotometrically. We used an acidification step to account for phaeopigments as suggested by Biggs and Kilroy (2000).

We used an Olympus (Tokyo, Japan) inverted microscope (CKX41) at 400× magnification to conduct biovolume

analyses. We used a color CCD camera (DP22, Olympus) to take 2 sets of 5 images along a vertical and horizontal transect giving a total of 10 images/sample. We made measurements for the estimation of cell dimensions with the DP22 controller software. We identified *Phormidium* to species level, whereas we identified all other algae to genus level (where possible), according to Biggs and Kilroy (2000). Where possible, we measured ≥30 cell lengths, widths, and heights and conducted biovolume calculations based on the suggested geometric shapes described by Olenina et al. (2006) and Hillebrand et al. (1999).

We analyzed $NO_3^- + NO_2^-$-N samples as NO_3^- after a spongy Cd reduction (Mackereth et al. 1978) and DRP by the molybdenum-blue method (APHA 2005). We measured all absorbances spectrophotometrically with a DR3900 spectrophotometer (Hach, Loveland, Colorado).

Statistical analyses

Accrual over time typically followed a nearly exponential increase, which in some cases was followed by an abrupt loss of area. We estimated the rates of increase for each cobble during the exponential phase as exponential accrual rate (EAR), by fitting a growth curve to the part of the accrued area vs time plot that exhibited exponential growth. For the fast treatments, we used days 1 to 16 for this expansion curve-fitting process. However, for the slow treatments, patch size was decreasing or stabilizing between days 11 and 16, and these points were excluded. Initially a simple exponential growth model was fitted to the patch data:

$$b = \frac{(lnN_2 - lnN_1)}{(t_2 - t_1)}, \qquad \text{(Eq. 2)}$$

where b is the EAR (1/d), lnN_2 is the natural log of patch size at time 2 (t_2) and lnN_1 is the natural log of patch size at time 1 (t_1).

However, this simplified model did not fit our data well because it tended to decrease over time. Therefore, we adopted a power function to model growth. This model provides an estimate of EAR at time 0 and includes a parameter that describes the rate at which EAR declines over time. We achieved better fits to our data with the power function. All treatments had R^2 values ≥0.81 (Table S1). The following growth model was used:

$$y = y0 + (atEAR)^{(1/a)}, \qquad \text{(Eq. 3)}$$

where y is the patch size (cm^2) at day t, $y0$ is the initial patch size at time $t = 0$, a is the decline parameter, and EAR is the exponential accrual rate at $t = 0$.

We tested for homogeneity of variances for the biomass accrual data by inspecting the residual and fitted values and with a Levene's test. We checked normality by inspecting quantile–quantile plots and with a Shapiro–Wilk test. We used a repeated-measures analysis of variance (ANOVA) to explore differences in clod-card dissolution between slow and fast velocity treatments. To evaluate the interactive effects of velocity and NO_3^- on biomass, we used 2-way ANOVAs. We undertook this analysis for phycoerythrin concentrations on day 16 only and days 4, 11, and 16 for Chl *a* and biovolume. We also used 2-way ANOVAs to test for difference in EAR among treatments. We calculated average EAR, Chl *a*, and phycoerythrin concentrations for each mesocosm individually from 3 sampled cobbles, and we used the averages for each of the 3 mesocosms for each treatment as replicates for 2-way ANOVAs. Type II sum of squares were used in the ANOVAs for Chl *a* and phycoerythrin concentrations. We identified and removed 2 outliers of >1.5× the interquartile range from the biovolume data set on day 16. This decision resulted in an unbalanced data set because only 1 sample was taken from each mesocosm. Therefore, we used Type III sum of squares in the 2-way ANOVA for the day-16 biovolume data. Where significant differences among treatments were identified by 2-way ANOVAs, we used post hoc (Tukey's Honest Significance Difference [HSD]) tests to identify which treatments were significantly different.

We visualized algal composition data via nonmetric multidimensional scaling (NMDS) based on Bray–Curtis similarity. We also used a permutational multivariate analysis of variance (PERMANOVA) to further examine changes in algal composition across the experimental period and among treatments.

We completed 2-way and repeated-measures ANOVAs with the software R Studio (version 3.1.1; R Project for Statistical Computing, Vienna, Austria) and all multivariate statistical tests with Primer (version 6.1; Primer-E Ltd., Plymouth, UK). We fitted growth models in SigmaPlot (Systat Software, San Jose, California).

RESULTS

Experimental conditions

Average NO_3^--N + NO_2^--N concentrations varied between 0.015 and 0.042, 0.089 and 0.141, and 0.375 to 0.494 mg/L for ambient, medium, and high nutrient treatments, respectively, throughout the experimental period (Table 1). Average DRP concentrations were similar among treatments and varied from 0.008 to 0.014 mg/L (Table 1). Clod-card dissolution was significantly different between slow and fast velocity treatments (repeated-measures ANOVA, $p < 0.05$; Fig. S1). The median mass lost was 4.9 and 7.9 g in slow and fast treatments, respectively. Average water temperature was consistent among mesocosms and varied from 11.6 to 15.0°C over the experimental period (Fig. S2).

Patch size and exponential accrual rate

Mean patch area increased over time in most treatments. The largest patch observed (65 cm^2) on day 16 was in the

FA treatment, and the smallest was in the SM treatment (14 cm^2) (Fig. 2A–F). EAR did not differ significantly among treatments (Tables 2, 3; range: 0.79–1.02 cm^2/d), but we observed an influence of velocity in the later accrual stages. Patches increased continually in size in fast treatments toward the end of the experimental period but either stabilized or decreased in size in slow treatments (Fig. 2A–F). The rate at which EAR decreased over time did not differ significantly among treatments (Tables 2, 3; range: 0.35–0.56).

Table 2. Mean (SD) calculated exponential accrual rates (EAR) and decline parameter (the rate at which EAR declined over time) for each treatment. See Table 1 for NO_3^- concentrations and Table S1 for model fits and errors associated with calculations.

Treatment	EAR (cm^2/d)	Decline parameter
Slow/ambient	1.02 (0.19)	0.56 (0.13)
Fast/ambient	0.79 (0.05)	0.35 (0.03)
Slow/medium	0.83 (0.28)	0.48 (0.17)
Fast/medium	0.83 (0.04)	0.49 (0.03)
Slow/high	0.84 (0.04)	0.51 (0.17)
Fast/high	0.90 (0.03)	0.49 (0.04)

Phormidium biomass among velocity and NO_3^- treatments

Average phycoerythrin concentrations, normalized to cobble size, differed significantly between velocity treatments and among NO_3^- treatments, and the velocity × NO_3^- interaction was significant (Table 3, Fig. 3). Mean phycoerythrin concentrations did not differ among slow treatments but did differ between the FA and FH and between FM and FH treatments (Tukey's HSD, $p < 0.001$; Fig. 3). Phycoerythrin concentrations, normalized to the size of the patch, followed a pattern similar to those normalized to the size of the cobble (Fig. S3).

Neither Chl *a* nor biovolume differed between velocity or NO_3^- treatments on days 4 and 11 (Table 3, Fig. 4A, B, D, E). On day 16, average Chl *a* concentrations varied from 13 mg/m^2 (SA) to 27 mg/m^2 (FH) (Fig. 4C). On day 16, Chl *a* concentrations tended to increase slightly with increasing velocity and NO_3^- concentrations. The NO_3^- effect was significant based on 2-way ANOVA (Table 3, Fig. 4C), but the Tukey's HSD test did not identify any statistically significant differences among treatments. In contrast, velocity and NO_3^- effects on *Phormidium* biovolumes were significant on day 16 (Table 3, Fig. 4B), and biovolumes were highest in fast velocity and high nutrient treatments. Post-hoc tests showed no significant difference in mean *Phormidium* biovolume between NO_3^- treatments at the same velocity, nor between velocity treatments at the same NO_3^- concentration, except at high NO_3^- (Tukey's HSD test, $p < 0.05$; Fig. 4F). Phycoerythrin concentrations and *Phormidium* biovolumes followed similar trends on day 16 and were correlated (adjusted $R^2 = 0.61$; Fig. S4).

Relative abundance of algal groups among treatments

All *Phormidium* within the mats was identified as *Phormidium autumnale* (hereafter *Phormidium*). *Phormidium* accounted for 39 (SM) to 57% (FA) of the total biovolume on day 4 (Fig. 5A). These values were lower (15.2 [SH] to 37% [FM]) on day 16, with a higher percentage measured in fast treatments (Fig. 5C). Green algae and other cyanobacteria generally composed <1% of the total biovolume on day 16, with green algae being more abundant earlier

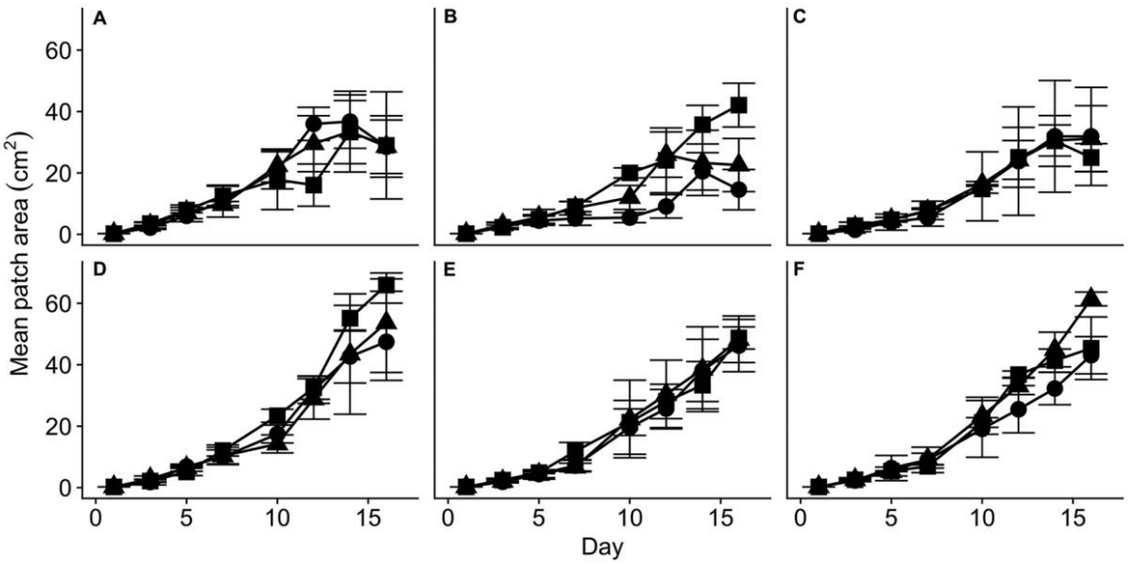

Figure 2. Mean (±SD, $n = 3$) *Phormidium* patch size in slow (A–C) and fast (D–F) velocity and ambient (A, D), medium (B, E), and high (C, F) NO_3^- treatments during the experimental period.

Table 3. Results of 2-way analyses of variance comparing exponential accrual rates (EAR), decline parameter (the rate at which EAR declined over time), and biomass estimates as phycoerythrin and chlorophyll *a* concentrations and biovolumes among treatments. Data that did not show exponential growth (days 11 and 16 in slow treatments) were removed. Significant *p* values (<0.05) are given in bold.

		Velocity treatment			NO_3^- treatment			Velocity × NO_3^-		
Variable	Day	df	*F*	*p*	df	*F*	*p*	df	*F*	*p*
EAR		1	0.80	0.39	2	0.43	0.66	2	1.83	0.20
Decline parameter		1	2.30	0.16	2	0.33	0.73	2	2.31	0.14
Phycoerythrin	Day 16	1	46.39	**<0.001**	2	9.08	**0.003**	2	3.88	**0.049**
Chlorophyll *a*	Day 4	1	2.53	0.14	2	2.17	0.16	2	1.40	0.30
	Day 11	1	0.008	0.98	2	3.39	0.07	2	0.58	0.56
	Day 16	1	0.156	0.70	2	4.45	**0.038**	2	2.46	0.13
Biovolume	Day 4	1	0.09	0.77	2	0.11	0.90	2	0.95	0.42
	Day 11	1	2.13	0.18	2	0.95	0.42	2	0.27	0.77
	Day 16	1	11.6	**<0.001**	2	5.70	**0.022**	2	2.14	0.17

in the experiment (Fig. 5B, C). Diatoms consisting of species of *Navicula*, *Synedra*, *Cymbella*, *Encyonema*, *Nitzschia*, and *Diatoma* were the most abundant algal group on days 11 and 16 across all treatments and made up 62 to 84% of the total biovolume (Fig. 5B, C). However, when the abundance of each genus was evaluated individually, *Phormidium* usually constituted the highest proportion of the total biovolume across treatments throughout the experiment (Fig. 6A–C). A 2-dimensional NMDS ordination showed a shift in taxonomic composition between day 4 and days 11 and 16 (Fig. 7). Community composition differed significantly over time but not between velocities or among NO_3^- treatments (PERMANOVA, $p < 0.001$).

Patch detachment dynamics between velocity treatments

The average number of *Phormidium* patches remaining at the end of the experiment was significantly higher in fast than in slow treatments (*t*-test, $p < 0.001$). An average of 7.8 patches survived in fast treatments, and 3.9 survived in slow treatments (Fig. 8A). Seventy-six percent of the patches that remained in the slow treatments on day 16 were partially detached (evidenced by decreases in the patch size). Less than 10% of patches in the fast treatments had decreased in fast treatments. The difference between the 2 treatments was significant (*t*-test, $p < 0.001$; Fig. 8B).

DISCUSSION

Most scientists investigating *Phormidium* dynamics at a reach scale have suggested that river flow and water-column NO_3^- play a role in determining its cover (Heath et al. 2011, Wood et al. 2017, McAllister et al. 2018), but the responses of individual patches to NO_3^- and velocity have not been assessed experimentally. We seeded cobbles with a standardized inoculum of *Phormidium*, which allowed high replication and examination of the effects of velocity and NO_3^- on the later 2 stages of the accrual cycle: expansion and detachment.

Patch expansion dynamics

Biomass accrual differed among treatments, but we did not identify any differences in initial expansion rates. Therefore, our 1st hypothesis was supported by biomass data but not expansion data. Patches did follow growth trajectories that differed between fast and slow-velocity treatments toward the end of the accrual cycle. By day 16, patches were larger in fast than in slow-velocity treatments because they

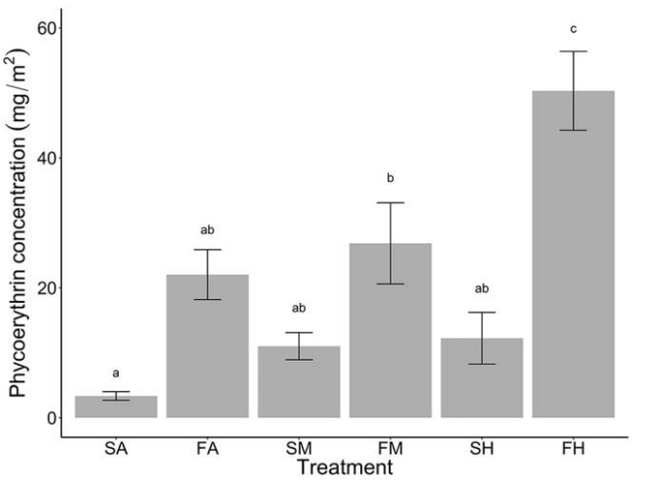

Figure 3. Mean (±SE) *Phormidium* phycoerythrin concentrations, normalized to cobble size, on day 16 of the experimental period. Bars with the same letter are not significantly different (Tukey's Honest Significant Difference, $p > 0.05$). SA = slow velocity/ambient NO_3^-, FA = fast velocity/ambient NO_3^-, SM = slow velocity/medium NO_3^-, FM = fast velocity/medium NO_3^-, SH = slow velocity/high NO_3^-, FH = fast velocity/high NO_3^-.

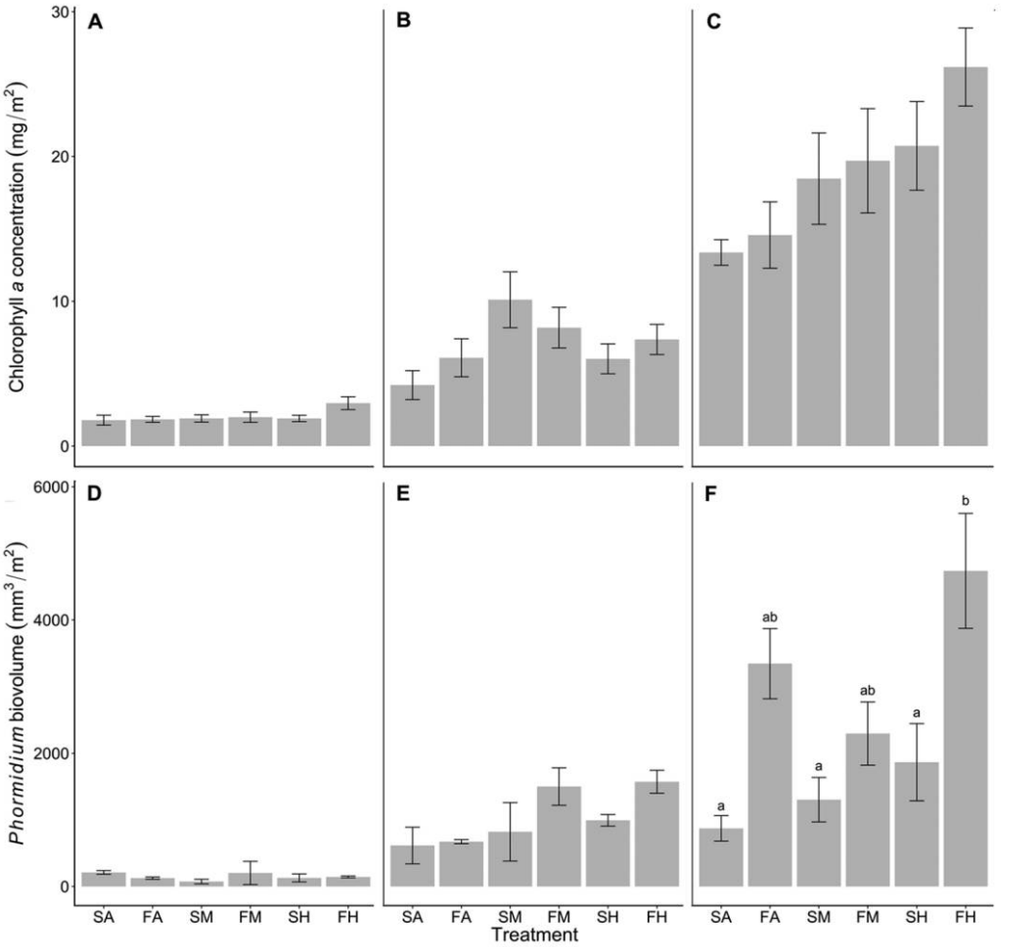

Figure 4. Mean (±SE) chlorophyll *a* (Chl *a*) concentrations (A–C) and *Phormidium* biovolumes (D–F) normalized to cobble size on days 4 (A, D), 11 (B, E), and 16 (C, F) of the experimental period. See Fig. 3 for treatment abbreviations.

maintained positive expansion for the 16-d experimental period. Our data were best modeled with a power function, which posits that, as patches enter the latter phase of their accrual cycle, expansion slows. The decline in exponential accrual rates occurred independently of treatments and was a function of patch size. The observed decrease or stabilization of growth in slow treatments toward the end of the experiment was not described by the growth models used in our study because they considered only the exponential growth phase. *Phormidium* patches in our experiment grew extremely quickly. For example, one patch grew from 0.3 to 65 cm^2 in 16 d, representing a 200-fold increase in patch size. This rapid growth could explain how proliferations form at the reach scale over a relatively short period of time.

Phormidium biomass accrual

The expansion rate in our study was velocity independent, in agreement with hypothesis 1. Velocity strongly affected *Phormidium* biovolumes and phycoerythrin concentrations, both of which were higher in fast-velocity treatments. As patches expanded, the expansion rate decreased, but phycoerythrin per unit area continued to increase, which suggests that cells were still growing at the same rate, but expanding more slowly laterally. The observed differences in phycoerythrin among treatments probably reflect both larger patches and thickening of patches. In some New Zealand rivers, *Phormidium* is strikingly patchy at the reach scale (McAllister et al. 2018). Variability in velocity may be one of the key factors causing this phenomenon. Biggs et al. (1998) provided evidence to support this idea for general periphyton, but highlighted that the effect of velocity depends on growth form. The growth form of *Phormidium*, which is a dense, low-profile, tightly adhering mucilaginous mat, should be advantageous in high velocity and should enable it to exploit these environments. Hart et al. (2013) noted that *Phormidium* was positively associated with velocity and generally was dominant at near-bed velocities of 0.4 m/s, whereas Heath

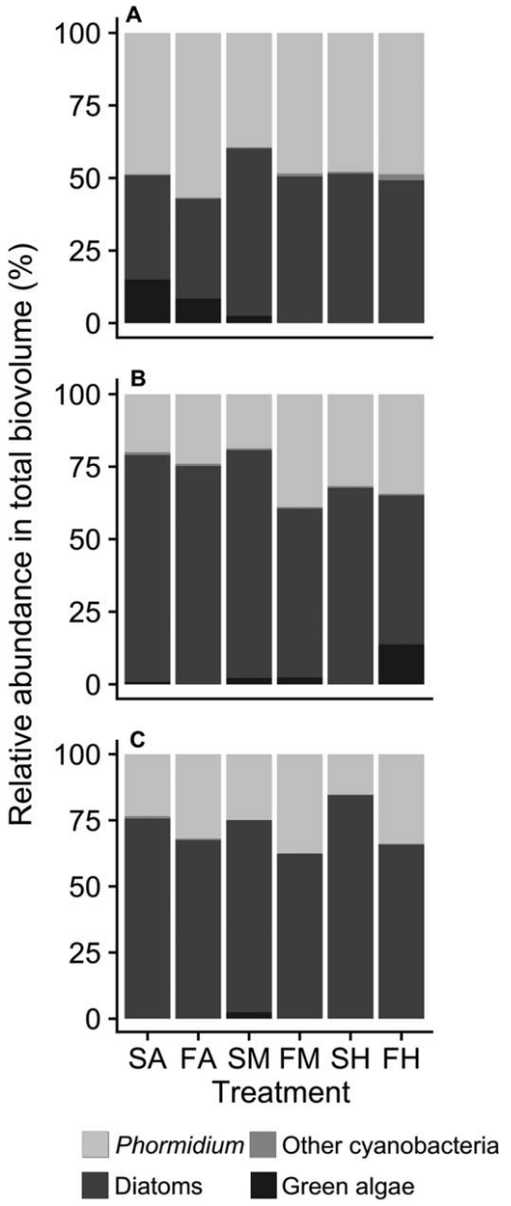

Figure 5. Algal taxonomic composition as % biovolume on days 4 (A), 11 (B), and 16 (C) of the experiment. See Fig. 3 for treatment abbreviations.

et al. (2015) found that cover was highest in velocities of 1 m/s. Hart et al. (2013) increased velocity in a manipulative field experiment and did not observe a change in *Phormidium* cover. However, this result may have been caused by the short-term nature of the experiment or the fact that patches were already in a late stage of accrual. The median velocity in run habitats in the Ōpihi River, where mats were collected, was ~0.2 m/s (TGM, unpublished data), so the fast-velocity treatment is representative of a run, rather than a riffle. Furthermore, the difference in velocity between fast and slow velocities in our study was only 0.1 m/s. This difference was enough to elicit a response, but we would expect that if the experimental system were capable of sustaining higher velocities, the differences in *Phormidium* biovolumes and phycoerythrin concentrations between the velocity treatments would have been greater.

Phycoerythrin concentrations showed similar patterns to *Phormidium* biovolumes across treatments, and these 2 biomass metrics were correlated. This correlation, in combination with the fact that patches did not differ in area and accrual rates during the early phase of the accrual cycle, suggests that patches increased in thickness and expanded laterally. However, this increase in thickness was a function of time and patch size and was independent of treatments.

Relationships between nutrients and algal biomass are thought to be most evident and important during early accrual stages (Sand-Jensen 1983) because exchanges between the water column and algal mat become less important as the mat develops and internal nutrient-cycling processes dominate. Conversely, in disagreement with hypothesis 2, we found that *Phormidium* did not show enhanced biomass accrual early in the experiment and that differences between treatments were most pronounced during late accrual stages. Seeding cobbles with *Phormidium* from established mats allowed high replication and standardization of starting biomass, but this approach probably had several ramifications for our experiments. If *Phormidium* biomass was not N limited, especially during early accrual, then NO_3^- would not have been required in high concentrations and, consequently, would not stimulate a response in biomass. The *Phormidium* used to seed cobbles was collected from established mats and may have taken up and stored N prior to collection, which could have contributed to growth early in the experiment. *Phormidium* biovolume increased up to 11-fold from days 4 to 11, and we think it unlikely that N stored prior to collection would have been sufficient to sustain this growth. Nutrient concentrations measured from water within *Phormidium* mats are often markedly different from those in the surrounding water column, possibly indicating internal nutrient cycling. For example, Wood et al. (2015) found that DRP concentrations in water within the *Phormidium* mat matrix were 300× higher than in the overlying water column. Martin (2017) found that total ammoniacal N concentrations were 40 to 200× higher in water within the *Phormidium* mat matrix than in bulk river water. The authors attributed this difference in ammoniacal N concentrations to N-fixing bacteria within *Phormidium* mats. *Phormidium* itself does not contain the genes required for N fixation, but these mats contain a variety of organisms, some of which are capable of fixing N (Heath 2009, Brasell et al. 2015). The established *Phormidium* mats we used to seed our cobbles could have already contained microbial communities capable of fixing N. Our observation of *Phormidium* proliferations at DIN concentrations <0.02 mg/L supports the assertion

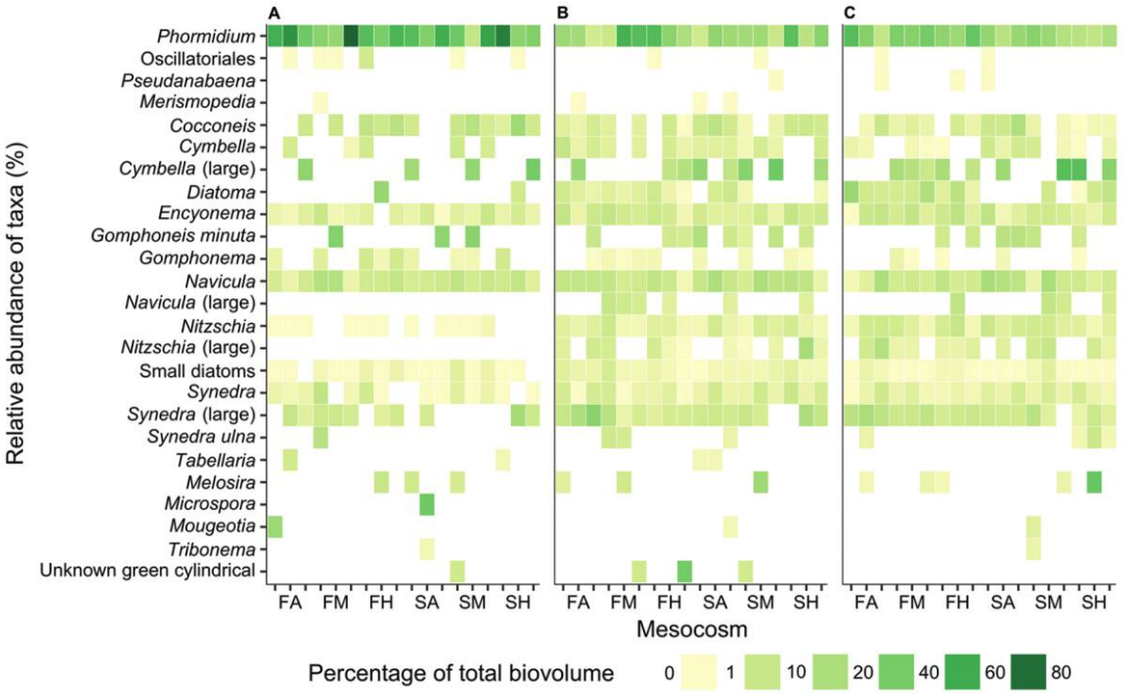

Figure 6. Relative abundance of taxa as % biovolume on days 4 (A), 11 (B), and 16 (C) of the experiment. See Fig. 3 for treatment abbreviations.

that N fixation could have been occurring (Heath et al. 2014, Wood et al. 2017, McAllister et al. 2018).

Our hypothesis that *Phormidium* biomass accrual would be positively related to increasing NO_3^- concentrations was not well supported. NO_3^- concentration had no effect on accrual rate, but a positive effect of NO_3^- on phycoerythrin concentrations was observed under high velocities, providing limited support for our 3rd hypothesis. *Phormidium* biovolume increased with NO_3^-, but the difference was not statistically significant. Phycoerythrin, like Chl *a*, is a protein

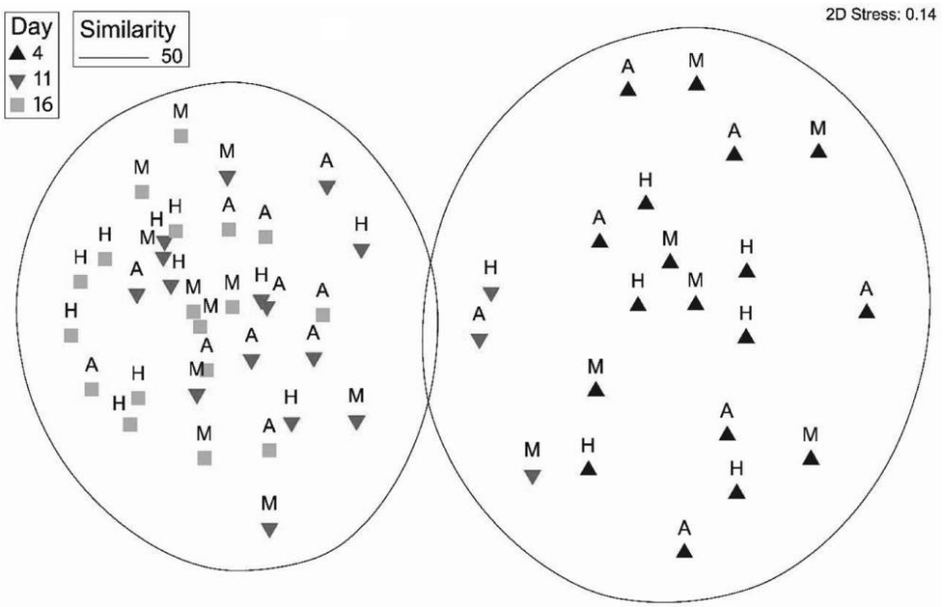

Figure 7. Two-dimensional nonmetric multidimensional scaling ordination based on Bray–Curtis similarities of biovolumes of cyanobacterial and algal communities in channels. Each data point displays one channel on the respective day. A = ambient, M = medium, and H = high nutrient concentrations.

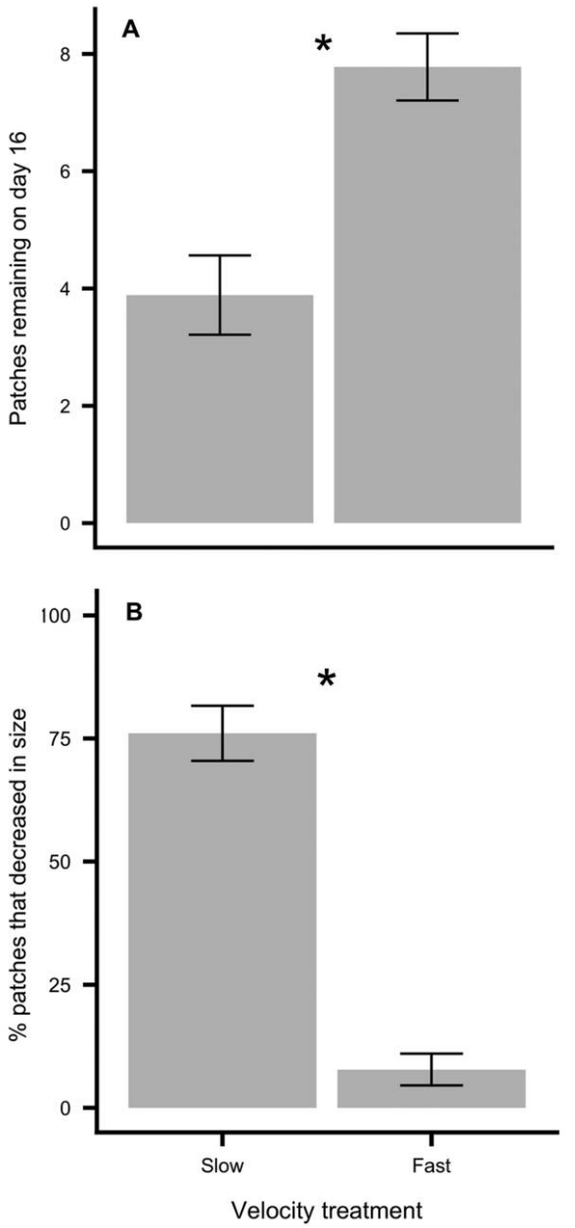

Figure 8. Mean (±SE) number of *Phormidium* patches remaining (A) and % patches that had decreased in size (B) by day 16 of the experimental period in slow and fast velocity mesocosms. * indicates a significant difference between treatments (*t*-test, $p < 0.001$).

that might be used to store N when it is in excess of growth requirements (Boussiba and Richmond 1980, Ördög et al. 2012). Therefore, an increase in phycoerythrin concentrations under high velocity with increasing NO_3^- could represent an increase in N storage. N was not limiting growth and other factors like light or temperature, which were relatively low throughout the experimental period, were limiting growth. Wood et al. (2017) highlighted that when DIN concentrations were <0.8 mg/L, DIN and *Phormidium* cover were positively related. Loza et al. (2014) found in a culture study that *Phormidium* responded positively to NO_3^- up to concentrations of 100 mg/L. Heath et al. (2016) in a similar culture study noted that cell concentrations decreased under reduced N concentrations. Our phycoerythrin results are in general agreement with previous research, but this effect was evident only in fast-velocity treatments. The mechanism underlying the positive effect of NO_3^- in fast velocities is likely to be related to boundary layers. The effect of the boundary layer would become more apparent as the mat develops and the boundary layer thickness increases (Sand-Jensen 1983). In fast velocity, the reduced thickness of the boundary layer might lead to an increase in NO_3^- delivery to the mat, resulting in increased biomass. In contrast, the effect of increasing NO_3^- in slow velocity is likely to be damped by the thickness of the boundary layer, thereby limiting NO_3^- delivery.

Chl *a* and algal composition

On day 16, we observed a general nonsignificant trend of increasing Chl *a* concentrations from slow to fast velocity and from ambient to high NO_3^- concentration. Chl *a* concentrations represent biomass of *Phormidium* patches and of other species. *Phormidium* was the dominant taxon, but diatoms (e.g., *Navicula*, *Synedra*, and *Cymbella*) composed a large proportion of the total biovolume, and this proportion increased throughout the experimental period. This shift in community composition was not attributable to changes in NO_3^- and velocity. Thus, a potential explanation for the lack of a significant relationship between Chl *a* and velocity is that Chl *a* is a proxy for the biomass of all photosynthetic organisms, whereas our other biomass metrics (phycoerythrin and biovolumes) were cyanobacteria/*Phormidium* specific (Echenique-Subiabre et al. 2016).

Chl *a* concentrations vary with community composition and environmental conditions, such as nutrients, light, and temperature (Kasprzak et al. 2008, Baulch et al. 2009), which makes its use as a proxy for biomass problematic. *Phormidium* mats are not composed only of this cyanobacterium; diatoms and green algae also can be abundant in mats (Hart et al. 2013, Brasell et al. 2015), and it is likely that this mixed assemblage may have masked differences of *Phormidium* biomass among treatments. Therefore, Chl *a* is not an appropriate metric for assessing *Phormidium* biomass accrual. We recommend assessing cyanobacteria-specific pigments or biovolumes in future studies.

Detachment

More *Phormidium* patches detached either partially or fully in slow- than fast-velocity treatments. This finding supports our 4th hypothesis that decreasing velocity would increase detachment. This result is similar to findings by Hart et al. (2013), who experimentally reduced velocity in a field

setting, which led to a decrease in *Phormidium* cover. One potential explanation for this phenomenon is accumulation of O_2 bubbles produced during photosynthesis within the mats. Bubbles trapped by the boundary layer can cause detachment of mats from the substrate (Boulêtreau et al. 2006). Bouma-Gregson et al. (2017) investigated the effects of bubbles on buoyancy and detachment processes of benthic *Anabaena* and found that the floating or sinking of mats was driven by O_2 production during photosynthesis, rather than by intracellular changes. Oxygen bubbles are often visible on *Phormidium* mats (Wood et al. 2017) and are likely to accumulate under slow-flow conditions (Boulêtreau et al. 2006, Bosak et al. 2010, Hawes et al. 2014). This effect can rapidly lead to sloughing of biomass and early termination of the accrual cycle, and mass mat-detachment events caused by this phenomenon have been observed (Sabater et al. 2003, Mendoza-Lera et al. 2016, McAllister et al. 2018). Understanding the drivers of detachment processes and causes of mass detachment is important because detached mats often accumulate at the edge of streams, places where animals and humans drink or undertake recreational activities, thereby increasing health risks.

Conclusions

Attempts to establish relationships between NO_3^- concentration, flow, and *Phormidium* cover in the field are complicated by covariation of other factors. Most laboratory studies were conducted in relatively static hydrodynamic conditions, which do not represent lotic systems. *Phormidium* accrual was greater in the fast- than in the slow-velocity treatment. This effect may have been enhanced had we been able to increase the velocity in the fast treatments. Our study also highlighted the rapidity with which *Phormidium* grows (0.3 to 65 cm^2 in 16 d [a 200× increase]). *Phormidium* biovolumes and phycoerythrin were positively related to NO_3^- concentration, but only in the fast-velocity treatment. Slow velocity resulted in increased detachment, which could mean increased dispersal and a higher associated health risk in a riverine system.

ACKNOWLEDGEMENTS

Author contributions: TGM, SAW, MJG, and IH designed the experiments. TGM, MJG, and FB performed experiments. TGM and FB conducted laboratory analyses. TGM, SAW, FB, and IH analyzed data. TGM, SAW, MJG, FB, and IH contributed materials/equipment. TGM, SAW, MJG, FB, and IH wrote the paper.

We thank Emma MacKenzie, Matthew Fraser, Channell Thoms, Anna Henderson, Olivia Rowley, Oliver Gooday, Mwangi Ruigu, Michael Knopick, and Qian Hu for assisting with field work. We thank the landowners for allowing access to the experimental facility and the National Institute of Water and Atmospheric Research, particularly Cathy Kilroy, for their assistance in conducting these experiments. TGM thanks the Ngāi Tahu Research Centre and Meadow Mushrooms for funding her PhD. Environment Canterbury funded our research. SAW received funding from the National Institute of Water and Atmospheric Research Ltd. under the Causes and Effects of Water Quality Degradation: Eutrophication Risk Assessment Programme.

LITERATURE CITED

Aboal, M., M. A. Puig, P. Mateo, and E. Perona. 2002. Implications of cyanophyte toxicity on biological monitoring of calcareous streams in north-east Spain. Journal of Applied Phycology 14:49–56.

APHA (American Public Health Association). 2005. Standard methods for the examination of water and wastewater. American Public Health Association, American Water Works Association, and Water Environment Federation, Washington, DC.

Baron, J. S., N. L. Poff, P. L. Angermeier, C. N. Dahm, P. H. Gleick, N. G. Hairston, R. B. Jackson, C. A. Johnston, B. D. Richter, and A. D. Steinman. 2002. Meeting ecological and societal needs for freshwater. Ecological Applications 12:1247–1260.

Baulch, H. M., M. A. Turner, D. L. Findlay, R. D. Vinebrooke, and W. F. Donahue. 2009. Benthic algal biomass—measurement and errors. Canadian Journal of Fisheries and Aquatic Sciences 66:1989–2001.

Biggs, B. J., D. G. Goring, and V. I. Nikora. 1998. Subsidy and stress responses of stream periphyton to gradients in water velocity as a function of community growth form. Journal of Phycology 34:598–607.

Biggs, B. J., and C. Kilroy. 2000. Stream periphyton monitoring manual. National Institute of Water and Atmospheric Research, Christchurch, New Zealand. (Available from: https://www.niwa.co.nz/sites/niwa.co.nz/files/import/attachments/peri_complete.pdf)

Bonilla, S., V. Villeneuve, and W. F. Vincent. 2005. Benthic and planktonic algal communities in a high arctic lake: pigment structure and contrasting responses to nutrient enrichment. Journal of Phycology 41:1120–1130.

Bosak, T., J. W. M. Bush, M. R. Flynn, B. Liang, S. Ono, A. P. Petroff, and M. S. Sim. 2010. Formation and stability of oxygen-rich bubbles that shape photosynthetic mats. Geobiology 8: 45–55.

Bothwell, M. L. 1988. Growth rate responses of lotic periphytic diatoms to experimental phosphorus enrichment: the influence of temperature and light. Canadian Journal of Fisheries and Aquatic Sciences 45:261–270.

Boulêtreau, S., F. Garabétian, S. Sauvage, and J. M. Sánchez-Pérez. 2006. Assessing the importance of a self-generated detachment process in river biofilm models. Freshwater Biology 51:901–912.

Bouma-Gregson, K. 2015. Cyanobacteria and cyanotoxins in the Eel River, 2013–2014. University of California, Berkeley, California. (Available from: http://www.eelriverrecovery.org/documents/ERRP_CyanoReport_18Aug2016_v2.pdf).

Bouma-Gregson, K., M. E. Power, and M. Bormans. 2017. Rise and fall of toxic benthic freshwater cyanobacteria (*Anabaena* spp.) in the Eel River: buoyancy and dispersal. Harmful Algae 66:79–87.

Boussiba, S., and A. E. Richmond. 1980. C-phycocyanin as a storage protein in the blue-green alga *Spirulina platensis*. Archives of Microbiology 125:143–147.

Brasell, K. A., M. W. Heath, K. G. Ryan, and S. A. Wood. 2015. Successional change in microbial communities of benthic *Phormidium*-dominated biofilms. Microbial Ecology 69:254–266.

Bryant, D. A., A. N. Glazer, and F. A. Eiserling. 1976. Characterization and structural properties of the major biliproteins of *Anabaena* sp. Archives of Microbiology 110:61–75.

Echenique-Subiabre, I., C. Dalle, C. Duval, M. W. Heath, A. Couté, S. A. Wood, J.-F. Humbert, and C. Quiblier. 2016. Application of a spectrofluorimetric tool (bbe BenthoTorch) for monitoring potentially toxic benthic cyanobacteria in rivers. Water Research 101:341–350.

Edwards, C., K. A. Beattie, C. M. Scrimgeour, and G. A. Codd. 1992. Identification of anatoxin-a in benthic cyanobacteria (blue-green algae) and in associated dog poisonings at Loch Insh, Scotland. Toxicon 30:1165–1175.

Faassen, E. J., L. Harkema, L. Begeman, and M. Lurling. 2012. First report of (homo) anatoxin-a and dog neurotoxicosis after ingestion of benthic cyanobacteria in The Netherlands. Toxicon 60:378–384.

Fetscher, A. E., M. D. A. Howard, R. Stancheva, R. M. Kudela, E. D. Stein, M. A. Sutula, L. B. Busse, and R. G. Sheath. 2015. Wadeable streams as widespread sources of benthic cyanotoxins in California, USA. Harmful Algae 49:105–116.

Gugger, M., S. Lenoir, C. Berger, A. Ledreux, J.-C. Druart, J.-F. Humbert, C. Guette, and C. Bernard. 2005. First report in a river in France of the benthic cyanobacterium *Phormidium favosum* producing anatoxin-a associated with dog neurotoxicosis. Toxicon 45:919–928.

Hamill, K. D. 2001. Toxicity in benthic freshwater cyanobacteria (blue-green algae): first observations in New Zealand. New Zealand Journal of Marine and Freshwater Research 35:1057–1059.

Hart, D. D., B. J. Biggs, V. I. Nikora, and C. A. Flinders. 2013. Flow effects on periphyton patches and their ecological consequences in a New Zealand river. Freshwater Biology 58:1588–1602.

Hawes, I., H. Giles, and P. T. Doran. 2014. Estimating photosynthetic activity in microbial mats in an ice-covered Antarctic lake using automated oxygen microelectrode profiling and variable chlorophyll fluorescence. Limnology and Oceanography 59:674–688.

Heath, M. W. 2009. Mat forming toxic benthic cyanobacteria in New Zealand: species diversity and abundance, cyanotoxin production and concentrations. MS Thesis, Victoria University, Wellington, New Zealand.

Heath, M. W., S. A. Wood, R. F. Barbieri, R. G. Young, and K. G. Ryan. 2014. Effects of nitrogen and phosphorus on anatoxin-a, homoanatoxin-a, dihydroanatoxin-a and dihydrohomoanatoxin-a production by *Phormidium autumnale*. Toxicon 92:179–185.

Heath, M. W., S. A. Wood, K. A. Brasell, R. G. Young, and K. G. Ryan. 2015. Development of habitat suitability criteria and instream habitat assessment for the benthic cyanobacteria *Phormidium*. River Research and Applications 31:98–108.

Heath, M. W., S. A. Wood, and K. G. Ryan. 2011. Spatial and temporal variability in *Phormidium* mats and associated anatoxin-a and homoanatoxin-a in two New Zealand rivers. Aquatic Microbial Ecology 64:69–79.

Heath, M. W., S. A. Wood, R. G. Young, and K. G. Ryan. 2016. The role of nitrogen and phosphorus in regulating *Phormidium* sp. (Cyanobacteria) growth and anatoxin production. FEMS Microbiology Ecology 92:fiw021.

Hillebrand, H., C. D. Dürselen, D. Kirschtel, U. Pollingher, and T. Zohary. 1999. Biovolume calculation for pelagic and benthic microalgae. Journal of Phycology 35:403–424.

Kasprzak, P., J. Padisák, R. Koschel, L. Krienitz, and F. Gervais. 2008. Chlorophyll *a* concentration across a trophic gradient of lakes: an estimator of phytoplankton biomass? Limnologica – Ecology and Management of Inland Waters 38:327–338.

Larned, S. T., V. I. Nikora, and B. J. F. Biggs. 2004. Mass-transfer-limited nitrogen and phosphorus uptake by stream periphyton: a conceptual model and experimental evidence. Limnology and Oceanography 49:1992–2000.

Larned, S. T., and J. Stimson. 1996. Nitrogen-limited growth in the coral reef chlorophyte *Dictyosphaeria cavernosa*, and the effect of exposure to sediment-derived nitrogen on growth. Marine Ecology Progress Series 145:95–108.

Loza, V., E. Perona, J. Carmona, and P. Mateo. 2013. Phenotypic and genotypic characteristics of *Phormidium*-like cyanobacteria inhabiting microbial mats are correlated with the trophic status of running waters. European Journal of Phycology 48: 235–252.

Loza, V., E. Perona, and P. Mateo. 2014. Specific responses to nitrogen and phosphorus enrichment in cyanobacteria: factors influencing changes in species dominance along eutrophic gradients. Water Research 48:622–631.

Mackereth, F. J. H., J. Heron, and J. F. Talling. 1978. Water analysis: some revised methods for limnologists. Freshwater Biological Association, Ambleside, UK.

Martin, E. 2017. Understanding the hydrological and physicochemical drivers of *Phormidium* proliferation in the Hutt and Waipoua Rivers. MS Thesis, Victoria University of Wellington, Wellington, New Zealand.

McAllister, T. G., S. A. Wood, J. Atalah, and I. Hawes. 2018. Spatiotemporal dynamics of *Phormidium* cover and anatoxin concentrations in eight New Zealand rivers with contrasting nutrient and flow regimes. Science of the Total Environment 612:71–80.

McAllister, T. G., S. A. Wood, and I. Hawes. 2016. The rise of toxic benthic *Phormidium* proliferations: a review of their taxonomy, distribution, toxin content and factors regulating prevalence and increased severity. Harmful Algae 55:282–294.

Mendoza-Lera, C., L. L. Federlein, M. Knie, and M. Mutz. 2016. The algal lift: buoyancy-mediated sediment transport. Water Resources Research 52:108–118.

Mez, K., K. A. Beattie, G. A. Codd, K. Hanselmann, B. Hauser, H. Naegeli, and H. R. Preisig. 1997. Identification of a microcystin in benthic cyanobacteria linked to cattle deaths on alpine pastures in Switzerland. European Journal of Phycology 32:111–117.

Olenina, I., S. Hajdu, L. Edler, A. Andersson, N. Wasmund, S. Busch, J. Gobel, S. Gromisz, S. Huseby, M. Huttunen, A. Jaanus, P. Kokkonen, I. Ledaine, and E. Niemkiewicz. 2006. Biovolumes and size-classes of phytoplankton in the Baltic Sea. Baltic Sea Environment Proceedings 106:1–44.

Oliver, R. L., D. P. Hamilton, J. D. Brookes, and G. G. Ganf. 2012. Physiology, blooms and prediction of planktonic cyanobacteria. Pages 155–194. Ecology of cyanobacteria II. Springer, Dordrecht, The Netherlands.

Ördög, V., W. A. Stirk, P. Bálint, J. van Staden, and C. Lovász. 2012. Changes in lipid, protein and pigment concentrations in nitrogen-stressed *Chlorella minutissima* cultures. Journal of Applied Phycology 24:907–914.

Quiblier, C., S. Wood, I. Echenique-Subiabre, M. Heath, A. Villeneuve, and J.-F. Humbert. 2013. A review of current knowledge on toxic benthic freshwater cyanobacteria–ecology, toxin production and risk management. Water Research 47:5464–5479.

Sabater, S., E. Vilalta, A. Gaudes, H. Guasch, I. Muñoz, and A. Romani. 2003. Ecological implications of mass growth of benthic cyanobacteria in rivers. Aquatic Microbial Ecology 32: 175–184.

Sand-Jensen, K. 1983. Physical and chemical parameters regulating growth of periphytic communities. Pages 63–71 *in* Robert G. Wetzel (editor). Periphyton of freshwater ecosystems. Springer, Dordrecht, The Netherlands.

Thompson, T. L., and E. P. Glenn. 1994. Plaster standards to measure water motion. Limnology and Oceanography 39:1768–1779.

Vörösmarty, C. J., P. B. McIntyre, M. O. Gessner, D. Dudgeon, A. Prusevich, P. Green, S. Glidden, S. E. Bunn, C. A. Sullivan, C. Reidy Liermann, and P. M. Davies. 2010. Global threats to human water security and river biodiversity. Nature 467:555–561.

Walling, D., and D. Fang. 2003. Recent trends in the suspended sediment loads of the world's rivers. Global and Planetary Change 39:111–126.

Weijters, M. J., J. H. Janse, R. Alkemade, and J. Verhoeven. 2009. Quantifying the effect of catchment land use and water nutrient concentrations on freshwater river and stream biodiversity. Aquatic Conservation: Marine and Freshwater Ecosystems 19: 104–112.

Wood, S. A., J. Atalah, A. Wagenhoff, L. Brown, K. Doering, R. G. Young, and I. Hawes. 2017. Effect of river flow, temperature, and water chemistry on proliferations of the benthic anatoxin-producing cyanobacterium *Phormidium*. Freshwater Science 36:63–76.

Wood, S. A., C. Depree, L. Brown, T. McAllister, and I. Hawes. 2015. Entrapped sediments as a source of phosphorus in epilithic cyanobacterial proliferations in low nutrient rivers. PLoS ONE 10:e0141063.

Wood, S. A., A. I. Selwood, A. Rueckert, P. T. Holland, J. R. Milne, K. F. Smith, B. Smits, L. F. Watts, and C. S. Cary. 2007. First report of homoanatoxin-a and associated dog neurotoxicosis in New Zealand. Toxicon 50:292–301.